

Weak-coupling Bardeen-Cooper-Schrieffer superconductivity in the electron-doped cuprate superconductors

L. Shan,^{1,*} Y. Huang,¹ Y. L. Wang,¹ Shiliang Li,² Jun Zhao,² Pengcheng Dai,^{2,3} Y. Z. Zhang,¹ C. Ren,¹ and H. H. Wen^{1,†}

¹National Laboratory for Superconductivity, Institute of Physics and Beijing National Laboratory for Condensed Matter Physics, Chinese Academy of Sciences, P.O. Box 603, Beijing 100080, China

²Department of Physics and Astronomy, The University of Tennessee, Knoxville, Tennessee 37996-1200, USA

³Neutron Scattering Sciences Division, Oak Ridge National Laboratory, Oak Ridge, Tennessee 37831-6393, USA

(Received 12 September 2007; published 28 January 2008)

We use in-plane tunneling spectroscopy to study the temperature dependence of the local superconducting gap $\Delta(T)$ in electron-doped copper oxides with various T_c 's and Ce-doping concentrations. We show that the temperature dependence of $\Delta(T)$ follows the expectation of the Bardeen-Cooper-Schrieffer (BCS) theory of superconductivity, where $\Delta(0)/k_B T_c \approx 1.72 \pm 0.15$ and $\Delta(0)$ is the average superconducting gap across the Fermi surface, for all the doping levels investigated. These results suggest that the electron-doped superconducting copper oxides are weak-coupling BCS superconductors.

DOI: 10.1103/PhysRevB.77.014526

PACS number(s): 74.72.Jt, 74.45.+c, 74.50.+r

I. INTRODUCTION

The physics of conventional superconductors can be well understood by the Bardeen-Cooper-Schrieffer (BCS) theory of superconductivity. Within the BCS model, the superconducting gap $\Delta(T)$ is weakly temperature dependent at low temperatures, but closes rapidly to zero near T_c . In the weak-coupling limit, $\Delta(0)/k_B T_c$ is 1.76 for an isotropic gap and becomes slightly smaller for an anisotropic gap, where $\Delta(0)$ is the zero-temperature gap averaged over the entire Fermi surface. Since there is no generally accepted microscopic theory for high-transition temperature (high- T_c) copper oxides, it would be interesting to see if the BCS theory can, under certain conditions, describe the physics of some high- T_c cuprates. For hole-doped (*p*-type) materials, a pseudogap appears at the antinodal region and may compete with the superconducting gap on the Fermi surface.^{1,2} Electron-doped (*n*-type) copper oxides, on the other hand, have a much weaker pseudogap effect and, thus, provide a good opportunity to investigate the superconducting gap without the influence of “Fermi arc,” “nodal metal,” or “pseudogap.”¹⁻⁵ Using angle resolved photoemission spectroscopy and transport measurements, previous works have found that the Fermi surfaces in the *n*-type cuprates have two-band characteristics⁶⁻¹⁰ and the superconducting gap has the non-monotonic *d*-wave pairing symmetry.¹¹⁻¹³ Unfortunately, the superconducting gap of *n*-type cuprates is relatively small, and determination of its exact value over a large doping range is an experimental challenge.¹²⁻¹⁷ Previous estimates suggest that the superconducting pairing strength of the *n*-type cuprates is close to a weak-coupling regime in the optimally doped and overdoped regions.^{18,19} Furthermore, tunneling data suggest that the superconducting gap increases monotonically with decreasing doping levels, even in the underdoped regime.¹⁷ Although much is known about these electron-doped cuprates, there have been no systematic study of the superconducting gap as a function of electron doping.

In this paper, we present the point-contact spectra measured on *n*-type cuprates $\text{Nd}_{2-x}\text{Ce}_x\text{CuO}_{4-y}$ (NCCO) and

$\text{Pr}_{1-x}\text{LaCe}_x\text{CuO}_{4-y}$ (PLCCO) over a wide doping range. We find that the temperature dependence of the average gap follows the BCS predictions with a universal weak-coupling ratio for all doping levels investigated.

II. EXPERIMENT

High-quality single crystals of NCCO and PLCCO were grown by the traveling-solvent floating-zone technique. As grown, the crystals are not superconducting. By annealing the samples at different temperatures in pure Ar or vacuum, bulk superconductivity with different T_c 's can be obtained.²⁰ The detailed information of the superconducting phases studied in this work are presented in Table I. The in-plane point-contact junctions were made by approaching the Pt/Ir alloy or Au tips toward the (100) and/or (110) surfaces of the single-crystal samples (as discussed in this paper, there is no obvious difference between these two directions). The tip's preparation and the details of the experimental setup were described elsewhere.²¹ In order to obtain high-quality junctions with good reproducibility, the samples were carefully processed by nonaqueous chemical etching before being mounted on the point-contact device.¹⁰ For each superconducting phase, we repeated measurements many times at different locations on the sample surface and obtained the local superconducting gap Δ and transition temperature T_c , which vary slightly around the bulk values.

TABLE I. Main superconducting phases studied in this work.

Label	Annealing	T_c (K)	Formula
plcco-un21	Underdoped	21	$\text{Pr}_{0.88}\text{LaCe}_{0.12}\text{CuO}_{4-y}$
plcco-un24	Underdoped	24	$\text{Pr}_{0.88}\text{LaCe}_{0.12}\text{CuO}_{4-y}$
ncco-op25	Optimally doped	25	$\text{Nd}_{1.85}\text{Ce}_{0.15}\text{CuO}_{4-y}$
plcco-ov17	Overdoped	17	$\text{Pr}_{0.85}\text{LaCe}_{0.15}\text{CuO}_{4-y}$
plcco-ov13	Overdoped	13	$\text{Pr}_{0.85}\text{LaCe}_{0.15}\text{CuO}_{4-y}$

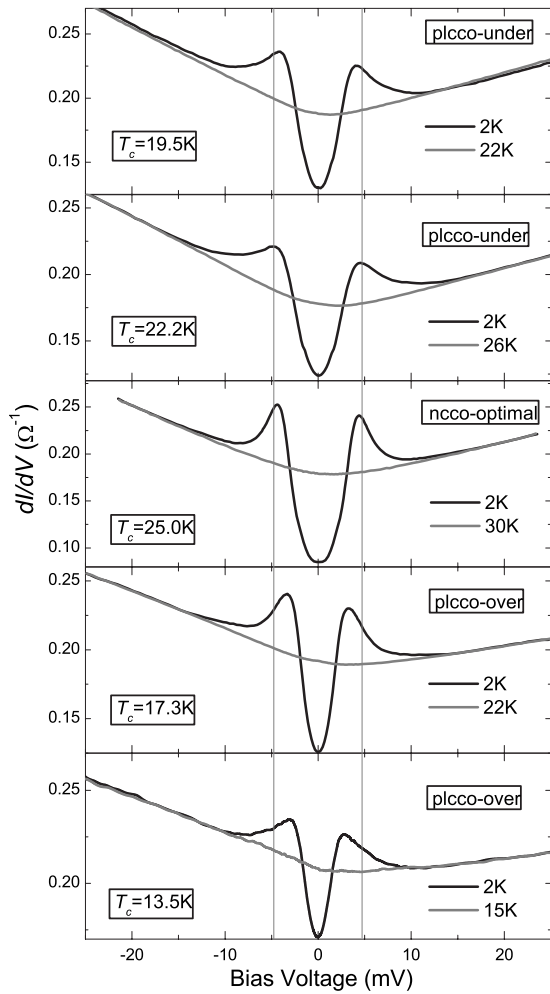


FIG. 1. Point-contact spectra measured at 2 K and well above T_c for various doping levels. The conductance drop has been subtracted from the spectra above T_c as explained in the text. Those two vertical gray lines are added as references to identify the positions of the coherence peaks.

III. RESULTS AND DISCUSSIONS

Figure 1 shows the point-contact spectra measured at various doping levels. These spectra are highly reproducible on the sample surface. In each run of the measurement, the spectra were recorded at various temperatures between 2 K and T_c , with increments of 1 K [refer to Figs. 3(a)–3(c)]. The data measured at $T=2$ K and well above T_c are presented in Fig. 1 for clarity. On the low temperature spectra, two coherence peaks are accompanied by low-energy depression of the quasiparticle density of states. The conductance within the gap voltage does not go to zero because the junctions are not tunnel junctions, but ballistic point-contact junctions with a finite tunneling barrier.^{22,23} One puzzling aspect of the data is that no zero bias conductance peak is found along the nodal direction for all doping levels, inconsistent with the expectation of nonmonotonic d -wave pairing symmetry for n -type cuprates.^{11–13,23} Instead, the spectra show almost identical shape with two distinct coherence peaks. This is difficult to understand within the current d -wave theory. This may be

caused by the microroughness (or corrugation) of the nodal surface arising from the inherent crystal-lattice structure and the axis dependent strength of chemical bonding. In this case, the dominated incident current is actually injected along the antinodal direction of the sample, and hence, the identical spectral shape for both nodal and antinodal directions can be easily understood.

It is well known that when temperature rises across the superconducting transition, the junction becomes normal and the background conductance drops notably due to a finite normal-state resistance of the sample (R_s) in series with the junction.²⁴ In this work, R_s varies from 0 to 2 Ω depending on the samples' property and the configuration of the electrodes and the point contacts. It can be subtracted simply by replacing dV/dI and V by $dV/dI - R_s$ and $V - IR_s$, respectively. All spectra (above T_c) shown in Fig. 1 have been treated in this way. Accordingly, we can readily construct a universal background and normalize the spectra below T_c , which were then compared with theoretical models. In addition to the rough estimation of 2Δ from the peak-to-peak distance of the spectra (it is well known that such method always overestimates the gap value when the measured spectrum is not ideal, in this work such overestimate can exceed 1 meV), we used the Blonder-Tinkham-Klapwijk (BTK) theory²² to derive Δ more accurately.^{25,26} In this model, two parameters are introduced to describe the effective potential barrier (Z) and the superconducting energy gap (Δ). As a supplement, the quasiparticle energy E is replaced by $E + i\Gamma$, where Γ is the broadening parameter characterizing the finite lifetime of the quasiparticles.^{27,28} For the extended anisotropic BTK model,²³ another parameter α was introduced to distinguish different tunneling directions. In this work, α is set to 0, corresponding to the antinodal direction as discussed above.

In Figs. 2(a) and 2(b), we present the comparison between the experimental data and the theoretical calculations for both isotropic and anisotropic BTK models. Figure 2(c) illustrates the gap function of the nonmonotonic d -wave pairing symmetry expressed explicitly by $\Delta_{anis} = \Delta_0 [1.43 \cos(2\phi) - 0.43 \cos(6\phi)]$.^{12,13} In some cases, the nodal region (the gray segments) has negligible contribution compared to the antinodal region (the black segments) because of the weaker spectral weight⁶ or fewer charge carriers^{8,10} possessed by the nodal Fermi pockets. As the first order approximation, we only consider the contribution from the antinodal region and describe the weakly angle dependent gap as a constant value, which is equal to the isotropic BTK model. As shown in Fig. 2(a), both the isotropic BTK model and the nonmonotonic d -wave one fit the data very well, possibly due to the broadening effect (a finite Γ value). If we look at the spectra shown in Fig. 2(b), which has a smaller broadening effect ($\Gamma/\Delta \approx 0.28$) than that in Fig. 2(a) ($\Gamma/\Delta \approx 0.44$), the nonmonotonic d -wave model fits the data better at higher energy outside the coherence peaks, while the isotropic model is more favorable at lower energy. This is consistent with the above discussions, i.e., the contribution from the antinodal Fermi pockets is dominant in this spectrum and the constant gap is a good approximation. In Fig. 2(d), we present the temperature dependence of the averaged

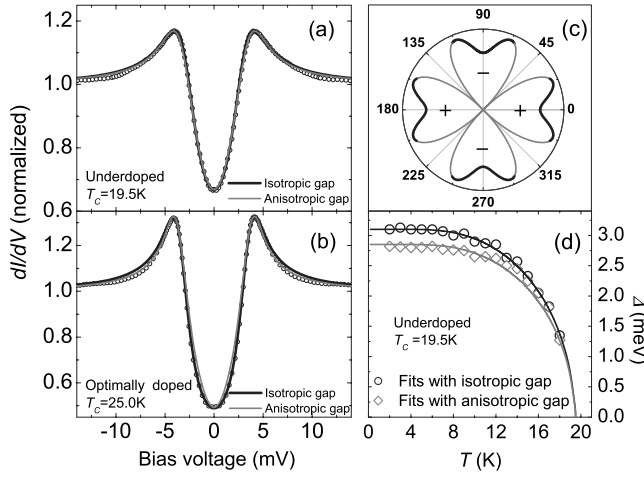


FIG. 2. Comparison of experimental data and theoretical calculations with the isotropic BTK model (black lines) and the anisotropic one (gray lines) for two samples: (a) plcco-un21 and (b) ncco-op25. (c) The schematic diagram of the anisotropic gap (or nonmonotonic d -wave gap), in which the black fragments indicate the antinodal region and the gray fragments indicate the nodal region. (d) Δ (averaged gap) $\sim T$ relations determined with two different models; solid lines are guides for the eyes.

superconducting gap determined by both models. We find that the averaged gap determined by the isotropic model has a very small uncertainty below 10% for all the doping levels.

Figure 3 illustrates the details of our data analysis. Figures 3(a)–3(c) show the temperature dependence of the normalized spectra of an underdoped sample, the optimally doped one, and an overdoped one, respectively. These data are consistent with the calculations based on the isotropic BTK model (denoted by the solid lines). As shown in Figs. 3(d)–3(i), the value of the fitted barrier strength (Z) lies between 1.0 and 1.5, and Γ value changes in a range from 0.7 to 1.5 meV without an obvious dependence on the doping levels. The independence of Z on temperature indicates high stability of the junctions. For the optimally doped and overdoped samples, Γ is also almost independent of temperature and increases with junction resistance similar to that of conventional BCS superconductors such as Nb (Ref. 30) and Zn.³¹ However, the Γ value of the underdoped sample decreases continuously when temperature increases very close to T_c . The temperature dependence of Γ may be closely related to the inhomogeneity, impurities, disorders, and scattering mechanism in this system, which need to be clarified by future experiments. In fact, it has been demonstrated that the Γ value is not an obstacle to derive the gap value for a wide temperature scope.¹⁰ For example, when Γ just exceeds Δ ($\Gamma/\Delta \approx 1.1$), the uncertainty of Δ is still below 30%. However, there is another factor making the fitting procedure more difficult, which was called “critical current effect,”³² because it will distort the shape of the spectra around T_c . Therefore, the upper temperature limit of our analysis is mainly determined by such effect. Accordingly, in some cases, we gave up fitting the spectra for the temperatures very close to T_c .

It is generally accepted that a practical point-contact junction often includes many channels or real point contacts, so it

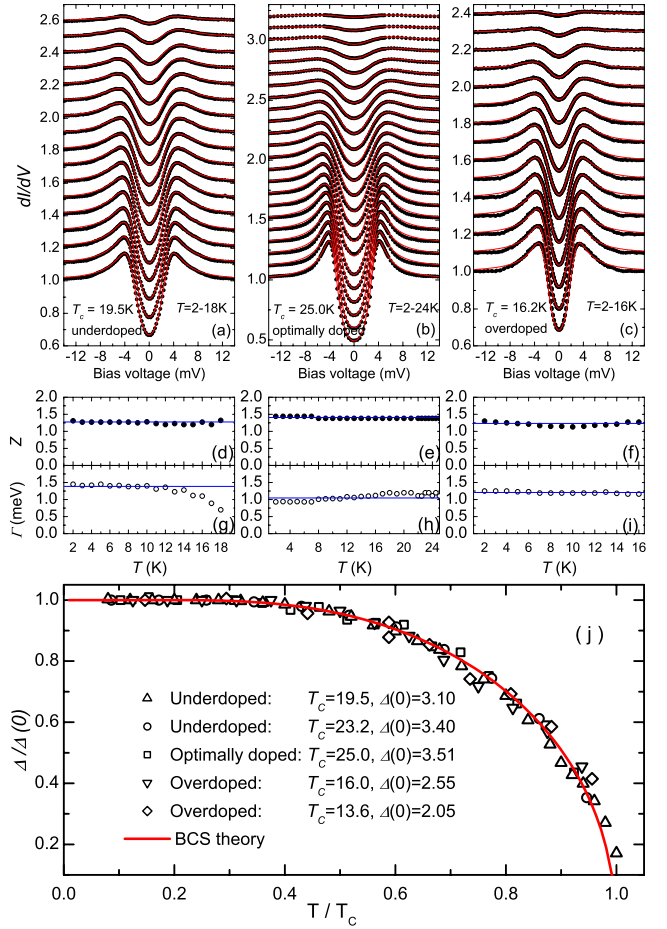


FIG. 3. (Color online) Temperature dependence of the normalized spectra (black dots) and theoretical calculations with the isotropic BTK model (solid lines) for (a) plcco-un21, (b) ncco-op25, and (c) plcco-ov17; all curves except the lowest one are shifted upward for clarity. (d)–(f) Fitting parameter of Z corresponding to the data shown in (a)–(c), respectively. (g)–(i) Fitting parameter of Γ corresponding to the data shown in (a)–(c), respectively. (j) The temperature dependence of the superconducting gap in a reduced scale for various doping levels.

is difficult to estimate the contact area simply according to the Sharvin formula. Alternatively, we have taken a prudent way to keep our measurements away from artificial errors. As elaborated in a previous reference,³³ after the metal tip reaches the sample surface, the barrier layer is abraded at first and its thickness decreases slightly with increasing pressure. Consequently, the measured spectrum becomes sharper due to the weakening of quasiparticle scattering near the normal-metal/superconductor microconstriction, and the barrier strength also decreases. Further pressure of the tip on the sample surface may simply flatten the point (validating more real point-contact channels) over the same minimal thickness of a tenacious barrier layer. In this case, if no artificial effect shows up, there should be no obvious change on the measured spectrum in a range of junction resistance (i.e., the normalized spectra should be identical) until the junction is damaged eventually. All measurements are carefully checked to be in such a regime. We have also found that the deter-

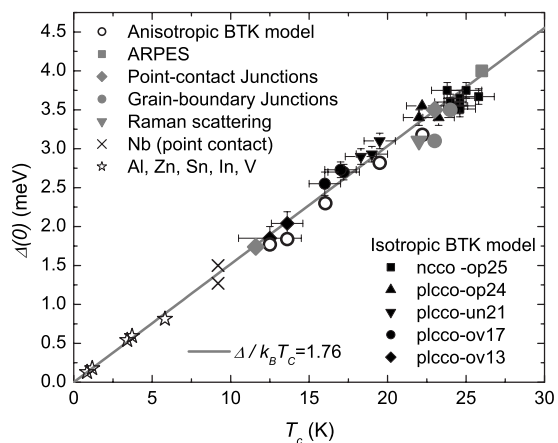


FIG. 4. Relationship between the zero-temperature averaged gap and transition temperature. The gray symbols indicate previous reports from ARPES (Ref. 13), Raman (Ref. 12), point contact (Ref. 16 and 17), and grain boundary (Ref. 14), respectively. The open circles denote the results of fitting to the nonmonotonic *d*-wave model. The crosses indicate the data of Nb measured by the same experimental apparatus used in this work. The data of some conventional superconductors are also presented as open stars for comparison (Ref. 29).

mined gap value is independent of the barrier strength and the measured locations (taking into account the slight variation of local T_c), indicating that we stood a good chance in detecting the bulk properties of the samples.

The temperature dependence of the superconducting gap is presented in Fig. 3(j) in a reduced scale. The universal $\Delta(T)$ relation was found for all studied doping levels in good agreement with the BCS theory. The derived $\Delta(0)$ and T_c for various locations on different samples are summarized in Fig. 4. For comparison, we also replot the data in previous reports^{12–14,16,17} (gray symbols) for optimally doped samples and an overdoped one. The coupling ratio is almost a con-

stant, with a value around 1.7. If the nonmonotonic *d*-wave model is used, this ratio becomes about 1.6 (as exemplified by the open circles). Both cases belong to the weak-coupling regime. As an example to demonstrate the validity of the methodology for determining the superconducting gap, we also presented in Fig. 4 the data from Nb-tip/Au-foil point contacts using the same experimental apparatus. The determined coupling ratio is consistent with previous reports²⁹ and BCS theory with a high precision.

IV. SUMMARY

In summary, by investigating the point-contact spectra of the electron-doped cuprates, we show that the temperature dependence of the superconducting gap follows the BCS prediction very well in a wide doping regime with a universal weak coupling ratio of $\Delta(0)/k_B T_c = 1.72 \pm 0.15$. Therefore, the electron-doped cuprates are weak-coupling BCS superconductors, although the nonmonotonic *d*-wave pairing symmetry may be favorable.

Note added. Recently, we became aware that a recent report indicates the weak-coupling BCS dirty superconductivity in an electron-doped cuprate based on the measurements of SIS' junctions.³⁴ We also became aware of a recent scanning tunneling microscopy paper³⁵ reporting larger gaps than that in this work.

ACKNOWLEDGMENTS

This work is supported by the National Science Foundation of China, the Ministry of Science and Technology of China (973 Projects No. 2006CB601000, No. 2006CB921802, and No. 2006CB921300), and Chinese Academy of Sciences (Project ITSNEM). The PLCCO and NCCO single-crystal growth at UT are supported by the U.S. DOE BES under Contract No. DE-FG-02-05ER46202. We acknowledge fruitful discussions with Zhi-Xun Shen and N. Nagaosa.

*shanlei@ssc.iphy.ac.cn

†hhwen@aphy.iphy.ac.cn

¹A. Damascelli, Z. Hussain, and Z. X. Shen, *Rev. Mod. Phys.* **75**, 473 (2005), and references therein.

²G. Deutscher, *Rev. Mod. Phys.* **77**, 109 (2005).

³Hai-Hu Wen, Lei Shan, Xiao-Gang Wen, Yue Wang, Hong Gao, Zhi-Yong Liu, Fang Zhou, Ji Wu Xiong, and Wenxin Ti, *Phys. Rev. B* **72**, 134507 (2005).

⁴M. R. Norman, D. Pines, and C. Kallin, *Adv. Phys.* **54**, 715 (2005).

⁵A. Kanigel, M. R. Norman, M. Randeria, U. Chatterjee, S. Suoma, A. Kaminski, H. M. Fretwell, S. Rosenkranz, M. Shi, T. Sato, T. Takahashi, Z. Z. Li, H. Raffy, K. Kadowaki, D. Hinks, L. Ozyuzer, and J. C. Campuzano, *Nat. Phys.* **2**, 447 (2006).

⁶N. P. Armitage, F. Ronning, D. H. Lu, C. Kim, A. Damascelli, K. M. Shen, D. L. Feng, H. Eisaki, Z.-X. Shen, P. K. Mang, N. Kaneko, M. Greven, Y. Onose, Y. Taguchi, and Y. Tokura, *Phys.*

Rev. Lett. **88**, 257001 (2002).

⁷Qingshan Yuan, Yan Chen, T. K. Lee, and C. S. Ting, *Phys. Rev. B* **69**, 214523 (2004).

⁸H. G. Luo and T. Xiang, *Phys. Rev. Lett.* **94**, 027001 (2005).

⁹C. S. Liu, H. G. Luo, W. C. Wu, and T. Xiang, *Phys. Rev. B* **73**, 174517 (2006).

¹⁰L. Shan, Y. Huang, H. Gao, Y. Wang, S. L. Li, P. C. Dai, F. Zhou, J. W. Xiong, W. X. Ti, and H. H. Wen, *Phys. Rev. B* **72**, 144506 (2005).

¹¹C. C. Tsuei and J. R. Kirtley, *Phys. Rev. Lett.* **85**, 182 (2000).

¹²G. Blumberg, A. Koitzsch, A. Gozar, B. S. Dennis, C. A. Kendziora, P. Fournier, and R. L. Greene, *Phys. Rev. Lett.* **88**, 107002 (2002).

¹³H. Matsui, K. Terashima, T. Sato, T. Takahashi, M. Fujita, and K. Yamada, *Phys. Rev. Lett.* **95**, 017003 (2005).

¹⁴S. Kleefisch, B. Welter, A. Marx, L. Alff, R. Gross, and M. Naito, *Phys. Rev. B* **63**, 100507(R) (2001).

- ¹⁵S. Kashiwaya, T. Ito, K. Oka, S. Ueno, H. Takashima, M. Koyanagi, Y. Tanaka, and K. Kajimura, *Phys. Rev. B* **57**, 8680 (1998).
- ¹⁶Q. Huang, J. F. Zasadzinski, N. Tralshawala, K. E. Gray, D. G. Hinks, J. L. Peng, and R. L. Greene, *Nature (London)* **347**, 369 (1990).
- ¹⁷Amlan Biswas, P. Fournier, M. M. Qazilbash, V. N. Smolyaninova, Hamza Balci, and R. L. Greene, *Phys. Rev. Lett.* **88**, 207004 (2002).
- ¹⁸A. Zimmers, R. P. S. M. Lobo, N. Bontemps, C. C. Homes, M. C. Barr, Y. Dagan, and R. L. Greene, *Phys. Rev. B* **70**, 132502 (2004).
- ¹⁹M. M. Qazilbash, A. Koitzsch, B. S. Dennis, A. Gozar, Hamza Balci, C. A. Kendziora, R. L. Greene, and G. Blumberg, *Phys. Rev. B* **72**, 214510 (2005).
- ²⁰Hye Jung Kang, Pengcheng Dai, Branton J. Campbell, Peter J. Chupas, Stephan Rosenkranz, Peter L. Lee, Qingzhen Huang, Shiliang Li, Seiki Komiyama, and Yoichi Ando, *Nat. Mater.* **6**, 224 (2007), and references therein.
- ²¹L. Shan, H. J. Tao, H. Gao, Z. Z. Li, Z. A. Ren, G. C. Che, and H. H. Wen, *Phys. Rev. B* **68**, 144510 (2003).
- ²²G. E. Blonder, M. Tinkham, and T. M. Klapwijk, *Phys. Rev. B* **25**, 4515 (1982).
- ²³Y. Tanaka and S. Kashiwaya, *Phys. Rev. Lett.* **74**, 3451 (1995); *Phys. Rev. B* **53**, 9371 (1996).
- ²⁴L. Alff, Y. Krockenberger, B. Welter, M. Schonecke, R. Gross, D. Manske, and M. Naito, *Nature (London)* **422**, 698 (2003).
- ²⁵H. Matsui, T. Sato, T. Takahashi, S.-C. Wang, H.-B. Yang, H. Ding, T. Fujii, T. Watanabe, and A. Matsuda, *Phys. Rev. Lett.* **90**, 217002 (2003).
- ²⁶J. E. Hoffman, K. McElroy, D.-H. Lee, K. M. Lang, H. Eisaki, S. Uchida, and J. C. Davis, *Science* **297**, 1148 (2002).
- ²⁷R. C. Dynes, J. P. Garno, G. B. Hertel, and T. P. Orlando, *Phys. Rev. Lett.* **53**, 2437 (1984).
- ²⁸A. Pleceník, M. Grajcar, Š. Beňačka, P. Seidel, and A. Pfuch, *Phys. Rev. B* **49**, 10016 (1994).
- ²⁹E. L. Wolf, *Principles of Electron Tunneling Spectroscopy* (Oxford University Press, New York, 1985).
- ³⁰L. Shan, Y. Huang, C. Ren, and H. H. Wen, *Phys. Rev. B* **73**, 134508 (2006).
- ³¹Yu. G. Naidyuk, H. v. Löhneysen, and I. K. Yanson, *Phys. Rev. B* **54**, 16077 (1996).
- ³²G. Sheet, S. Mukhopadhyay, and P. Raychaudhuri, *Phys. Rev. B* **69**, 134507 (2004).
- ³³G. E. Blonder and M. Tinkham, *Phys. Rev. B* **27**, 112 (1983).
- ³⁴Y. Dagan, R. Beck, and R. L. Greene, *Phys. Rev. Lett.* **99**, 147004 (2007).
- ³⁵F. C. Niestemski, S. Kunwar, S. Zhou, Shiliang Li, H. Ding, Ziqiang Wang, Pengcheng Dai, and V. Madhavan, *Nature (London)* **450**, 1058 (2007).